Journal of
Advanced Microscopy Research
Vol. 13, 1–9, 2018

Optimizing Chemical Vapor Deposition Parameters to Attain Minimum Diameter Carbon Nano Tubes by Response Surface Methodology

V. Sivamaran[1,*], V. Balasubramanian[2], M. Gopalakrishnan[3], V. Viswabaskaran[4], and A. Gouravrao[5]

[1] *Research Scholar, Centre for Materials Joining and Research (CEMAJOR), Department of Manufacturing Engineering, Annamalai University, 608002, India*
[2] *Centre for Materials Joining and Research (CEMAJOR), Department of Manufacturing Engineering, Annamalai University, 608002, India*
[3] *Department of Chemistry, Annamalai University, 608002, India*
[4] *VBCeramic Research Centre (VBCRC), Chennai 600041, India*
[5] *Scientist 'C', Naval Materials Research Laboratory (NMRL), 421506, India*

The MWCNTs (Multi walled carbon nano tubes) with diameter closer to SWCNTs (Single walled carbon nano tubes) found to have superior mechanical strength compared to the larger diameter of MWCNTs. Thermal chemical vapor deposition (CVD) process is widely used to synthesize multiwall carbon nano tubes. The main issue faced in the synthesis of carbon nano tubes (CNTs) via CVD process is the selection of optimum parameters for the growth of well aligned and required diameter of CNTs. This issue may be rectified by the correlating parameters of CVD process (reaction temperature, flow rate of precursor gas and process time) and the output product morphology of MWCNTs. The main aim of this research work is to optimize CVD process parameters to attain minimum diameter multi wall CNTs. For this purpose, statistical tools such as design of experiments, analysis of variance and response surface methodology were utilized. The FESEM (Field emission scanning electron microscopy) and HRTEM (High resolution transmission electron microscopy) techniques were used to study the characteristics of MWCNTs. The optimum CVD parameters were found at 1000 °C reaction temperature, 120 ml/min flow rate of precursor gas and 35 mins process time. This combination of parameters yielded a minimum diameter multiwall CNTs of 17 nm.

Keywords: Carbo Nano Tube, Chemical Vapor Deposition, Design of Experiments, Analysis of Variance.

RESEARCH ARTICLE

1. INTRODUCTION

The carbon nanotubes (CNTs) related businesses have grown abundantly during the past decade,[1] due to their unique mechanical[2] and electrical[3] properties. Compared to single walled carbon nanotubes (SWNTs), the cost of multiwalled carbon nanotubes (MWCNTs) was substantially low, because of their easy scalable production method.[4] So, one can replace the SWCNTs by MWCNTs in many applications, if there is no restriction in length, diameter and band gap of nanotubes. The MWCNTs were used in many emerging applications like composite materials,[5] thin film paint coating[6] etc. In some applications the mechanical strength is indeed to withstand a certain conditions, but due to their defect structure and also an increase in an outer diameter led to decrease in mechanical strength.[7] Hence, it is inevitable to synthesis MWCNTs with relatively close to SWCNTs diameter.

Chemical vapor deposition (CVD) has been recognized as one of the most promising technique for synthesizing large-scale carbon nano tubes (CNTs). CNTs have been produced by various methods, mainly including arc discharge,[8] laser ablation[9] and CVD[10] process. Compared with the other two methods, CVD is considered as the most promising method for easily scaled-up to batch-scale production due to simplicity and economy. The CVD methods are attractive because of their effectiveness in generating carbon feedstock and the straight forward scale up. Furthermore, it could be possible to achieve different types of CNTs by controlling various set of process parameters.[11,12]

Several factors may influence the structure of CNTs like reaction temperature,[13,14] process time,[15] and flow rate

*Author to whom correspondence should be addressed.

of precursor gas.[16] Predominantly, researchers around the world used COST (change one separate factor at a time) approach for optimization. The main disadvantage of this approach is, the amount of required experiments grows very fast with the number of variables and thus, the complete optimization of real systems is rather unfeasible.[17, 18]

The usage of conventional methods has many limitations compared to the response surface methodology (RSM). The RSM is used to identify the optimum operational conditions in a system, which satisfies all the required criteria.[19] The authors[13, 18–20] have studied the influence of CVD process parameters on yield, morphology and length of CNTs, but very few researches have carried out the experiments to examine the diameter of MWCNTs.

Therefore, the main aim of this investigation is to develop an empirical relationship to predict the diameter of the MWCNTs by the statistical design of experiments. A standard RSM design called a central composite design (CCD) was selected to simultaneously to study the effects of reaction temperature, process time and flow rate of precursor gas on the mean diameter of the carbon samples. Empirical relationship relating these preparation variables (reaction temperature (T), process time (P) and precursor gas flow rate (F)) to the response (mean diameter of MWCNTs) was then developed.

RESEARCH ARTICLE

2. EXPERIMENTAL DETAILS

In order to achieve the desired objective, the present investigation was planned in the following sequence:

1. Identify the important CVD process parameters;
2. Find the upper and lower limits of the identified parameters;
3. Choose the relevant experimental design matrix;
4. Prepare the required catalyst;
5. Conduct the experiments as per the design matrix;
6. Purify MWCNTs by wet chemistry method;
7. Measure the average diameter of MWCNTs;
8. Record the responses (average diameter of MWCNTs);
9. Formulate empirical relationship to predict the diameter of MWCNTs;
10. Perform numerical and graphical optimization.

2.1. Identify Important CVD Parameters and Their Levels

From the literature[17, 21, 22] it was identified that (i) reaction temperature (ii) precursor flow rate (iii) process time are the predominant CVD parameters influencing morphology and diameter of CNTs. From the trial experiments, the feasible working ranges of CVD parameters were identified and they are presented in Table I.

Generally, the central composite design (CCD) consists of 2^n factorial runs with $2n$ axial runs and n_c centre runs (six replicates). For each categorical variable, a 2^3 full factorial CCD for the three variables, consisting of eight factorial points, six axial points and six replicates at the centre points were employed; indicating that altogether 20 experiments were required, as calculated[18] from Eq. (1):

$$N = 2^n + 2n + n_c = 2^3 + 2 \times 3 + 6 = 20 \qquad (1)$$

Where N is the total number of experiments required and n is the number of variables.

The Table II shows the experimental design matrix of coded values and actual values of the CVD parameters. The centre points were used to determine the experimental error and the reproducibility of the data. The independent variables were coded to the $(-1, 1)$ interval where the low and high levels were coded as -1 and $+1$, respectively. The axial points were located at $(\pm 1.682, 0, 0)$, $(0, \pm 1.682, 0)$ and $(0, 0, \pm 1.682)$ where 1.682 is the distance of the axial point from the centre and makes the design rotatable.

Table I. Important CVD process parameters and their levels.

No.	Parameter	Notation	Unit	Levels				
				−1.682	−1.0	0	−1.0	1.682
1	Reaction temperature	T	°C	732	800	900	1000	1068
2	Flow rate of precursor gas	F	ml/min	106	120	140	160	174
3	Process time	P	mins	8	15	25	35	42

2.2. Catalyst Preparation

The second step of the experimental procedure is to prepare the required amount of catalyst according to the number of experiments to conduct and the amount of catalyst

Table II. Experimental design matrix and the results.

Expt. no.	Coded values			Actual values			Average diameter of MWCNTs (nm)
	T	F	P	T (°C)	F (ml/min)	P (mins)	
1.	−1.00	−1.00	−1.00	800	120	15	29
2.	1.00	−1.00	−1.00	1000	120	15	23
3.	−1.00	1.00	−1.00	800	160	15	31
4.	1.00	1.00	−1.00	1000	160	15	39
5.	−1.00	−1.00	1.00	800	120	35	22
6.	1.00	−1.00	1.00	1000	120	35	17
7.	−1.00	1.00	1.00	800	160	35	27
8.	1.00	1.00	1.00	1000	160	35	35
9.	−1.682	0	0	732	140	25	31
10.	1.682	0	0	1068	140	25	33
11.	0	−1.682	0	900	106	25	15
12.	0	1.682	0	900	174	25	32
13.	0	0	−1.682	900	140	8	33
14.	0	0	1.682	900	140	42	24
15.	0	0	0	900	140	25	32
16.	0	0	0	900	140	25	34
17.	0	0	0	900	140	25	33
18.	0	0	0	900	140	25	31
19.	0	0	0	900	140	25	32
20.	0	0	0	900	140	25	33

to be loaded in the CVD chamber per run. The NiO/Al_2O_3 catalyst was prepared by impregnating 1 g of fumed alumina nano particles with 0.245 g of $Ni(NO_3) \cdot 6H_2O$ in 30 ml of methanol solution. The impregnation typically lasts for 1 hour at room temperature using a magnetic stirrer. The methanol solution was removed via rotary evaporator and obtained material was then heated at 150 °C overnight followed by grinding into a fine powder. This resulting product,[12, 13] denoted as NiO/Al was used as catalyst in this investigation.

2.3. Synthesize MWCNTs

The MWCNTs were synthesized at atmospheric pressure in a quartz tube reactor (Diameter: 70 mm, Length: 300 mm) by thermal chemical vapor deposition machine. The synthesis of MWCNTs was carried out as per the conditions prescribed by the Table I. In these experimental conditions, the catalyst loading (10 mg) and carrier gas (Argon: 100 ml min^{-1}) flow rate were kept constant. The catalyst was loaded into the centre of the hot zone reactor and argon (100 ml min^{-1}) was switched on until reaching reaction temperature and then argon is switched off, then replaced by the carbon precursor (acetylene) to flow to the reaction zone according to the process time and acetylene was replaced with argon until the furnace reaches room temperature. The carbon samples along with catalyst particles were collected from the quartz tube for the purification process to remove amorphous carbon and catalyst particles.[12]

2.4. Purify MWCNTs

After CVD process, the samples were purified by three steps (i) acid treatment (ii) sonication and (iii) filtered in sintering ceramic crucible. In the acid treatment step, the samples (derived from CVD process) were stirred in concentrated nitric acid for three hours at room temperature. During this process of acid treatment carbon diffused samples, metal content was dissolved in the acid, but CNTs withstand the strong acid attack. After acid treatment, the metals (Catalysts particle) and amorphous carbon products were dissolved in acid solution due to the acid attack. The crystalline carbon products were free from catalyst[24–26] materials. The crystalline carbon samples were suspended in ethanol solution and sonicated for 10 mins. In this process the agglomerated particles separated and MWCNTs was filtered in sintering ceramic crucible and Carbon products were dried in a furnace.

2.5. Measuring the Average Diameter of MWCNTs

The MWCNTs synthesized by CVD process were characterized by the field emission scanning electron microscopy (FESEM) technique. FESEM images of MWCNTs synthesized using various combination of CVD parameters are shown in Figure 2, diameter of MWCNTs was measured using image analysis software at different locations and average diameter is presented in Table II.

3. DEVELOPING STATISTICAL MODELS

The obtained responses (diameter of MWCNTs) were incorporated into the design matrix (Actual: Table II) to develop an empirical relationship. The evaluation of model $f(x)$ is analyzed by selecting the quadratic order and polynomial model. To correlate the CVD parameters and average diameter of MWCNTs, a second order quadratic model was developed. The response 'D' (average diameter of MWCNTs) is a function of reaction temperature (T), precursor flow rate (F) and process time (P). Hence it can be expressed as,

$$D = f\{T, F, P\} \tag{2}$$

An empirical relationship was developed for each response that correlated to the CNT production variables using a second-degree polynomial equation as given by Eq. (3):

$$Y = b_0 + n\sum_{i=1} b_i x_i + \left(\sum_{i=1}^{n} b_i x_i\right)^2 + \sum_{i=1}^{n-1}\sum_{j=1}^{n} b_{ij} x_{ij} \tag{3}$$

Where Y is the predicted response, b_0 is the constant coefficient, b_i is the linear coefficients, b_{ij} is the interaction coefficients, b_{ii} is the quadratic coefficients and x_i, x_j are the coded values of the MWCNTs production variables.

For the three factors, the selected polynomial could be expressed as

$$D = \{b_0 + b_1(T) + b_2(F) + b_3(P) + b_{12}(TF) + b_{13}(TP) + b_{23}(FP) + b_{11}(T^2) + b_{22}(F^2) + b_{33}(P^2)\} \text{ nm} \tag{4}$$

Where b_0 is the average of response (mean diameter) and b_1, b_2, b_3, b_{12}, b_{13}, b_{23}, b_{11}, b_{22}, b_{33} are the coefficients of the respective main and interaction factors, which were calculated using the expression given below,

$$b_i = \sum(X_i, Y_j)/n \tag{5}$$

Where 'i' varies from 1 to n, in which X_i is the corresponding coded value of a factor and Y_j is the corresponding response output value (mean diameter) attained from experiment and 'n' is the total number of combinations considered. All the coefficients were calculated by applying central composite face centered design using the design expert statistic software package. The significance of each co-efficient was calculated by students t-test and p-values, which are presented in Table III. The value of "Prob > F" less than 0.05 indicate that the model terms are significant. The Model F-value of 137.93 implies the model is significant. There is only a 0.01% chance that a "Model F-value" this large could occur due to noise. Values of "Prob > F" less than 0.0500 indicate model terms are significant. In this case T, F, P, TF, FP, T^2, F^2, P^2 are significant model terms. Values greater than the model terms are not significant. If there are many insignificant model terms (not counting those required to support

RESEARCH ARTICLE

Table III. ANOVA test results.

Source	Sum of squares	df	Mean square	*F* value	*p*-value prob > *F*
Model	710.48	9	78.94	137.93	<0.0001 significant
T	5.12	1	5.12	8.95	0.0135
F	354.61	1	354.61	619.60	<0.0001
P	95.62	1	95.62	167.07	<0.0001
TF	91.13	1	91.13	159.22	<0.0001
TP	0.13	1	0.13	0.22	0.6503 insignificant
FP	3.13	1	3.13	5.46	0.0416 insignificant
T^2	0.31	1	0.31	0.53	0.4819
F^2	143.06	1	143.06	249.98	<0.0001
P^2	27.56	1	27.56	48.16	<0.0001
Residual	5.72	10	0.57		
Lack of fit	0.22	5	0.045	0.041	0.9984 not significant
Pure error	5.50	5	1.10		
Corrected total	716.20	19			

Notes: df: Degrees of freedom; CV: Coefficient of variation; *F*: Fisher ratio; *P*: Probability.

hierarchy), model reduction may improve our model. The "Predicted *R*-squared" of 0.9863 is in reseasonable agreement with the "Adjusted *R*-squared" of 0.9848.

After determining the significant coefficients (at 95% confidence level), the final relationship was developed using these coefficients. The final empirical relationship derived by the above method, to estimate the mean diameter of MWCNTs synthesize by CVD process is given below,

$$\begin{aligned}\text{Mean Diameter of MWCNTs} &= \{49.48371 - 0.20705(T) + 0.86344(F) - 0.12311(P) \\ &\quad + 0.00168(TF) + 0.000125(TP) + 0.00312(FP) \\ &\quad - 0.000015(T^2) - 0.00787(F^2) - 0.013830(P^2)\}\ \text{nm}\end{aligned} \tag{6}$$

Fig. 1. Photograph of CVD set up.

Where *T* is the coded value of the reaction temperature, *F* is the coded value of the Flow rate of Precursor gas and *P* is the coded value of the Process Time. A positive sign in front of the terms indicates synergistic effect, whereas a negative sign indicates an antagonistic effect.

4. RESULTS AND DISCUSSION

The surface morphology and growth structure of CNTs was analyzed using FESEM images. The Figure 2 illustrates the CNTs synthesized by CVD process for different set of experiments as per the design matrix. The Figure 2(a) represents the MWCNTs that relatively synthesized using the conditions prescribed by experiment number 4 and the diameter distribution ranges from 30 to 43 nm. From Figure 2(a), it could be observed that the walls of the CNTs were coated with amorphous carbon and also found presence of inactivated catalyst. The Figure 2(b) represents the MWCNTs synthesized using the conditions prescribed by the 5th experiment and the diameter distribution ranges from 17 to 26 nm. From Figure 2(b), it could be observed that the presence of bundled and also amorphous carbon in the CNTs sample. The Figure 2(c) represents the MWCNTs synthesized for the exp. no. 6 and the diameter distribution ranges from 13 to 22 nm. From the Figure 2(c), the presence of bundles and individual CNTs were observed. The Figure 2(d) represents the MWCNTs synthesized for the exp. no. 14 and the diameter distribution ranges from 18 to 25 nm. From the image 2(d), it could be observed that the presence of only CNTs bundles, abundant amorphous carbon and inactivated catalyst particles.

The perturbation plot is found to be the perfect schematic representation to study the effect of process variables individual effect on the response, so the developed empirical relationships can be used in actual fact to predict the responses by substituting process parameter values in coded form. Based on these empirical relationships, the main and interaction effects of the process parameters on the diameter of MWCNTs were computed and plotted in the form of perturbation plots, as shown in Figure 3. The perturbation plot helps to compare the effect of all the factors at a particular point in the design space. The steep slope or curvature in a factor shows that the response is sensitive to that factor. A relatively flat lines shows insensitivity to change in that particular factor. The Figure 3 shows the perturbation graph for mean diameter of MWCNTs and its interaction effect with process factors. The perturbation plots of the responses are presented with the purpose of understanding the main and interaction effects of each factor, considering the full quadratic model. The average diameter has been plotted as a function of the normalized independent variables. It is found that the flow rate of precursor gas has the most significant effect on the mean diameter of MWCNTs. However, the effects

RESEARCH ARTICLE

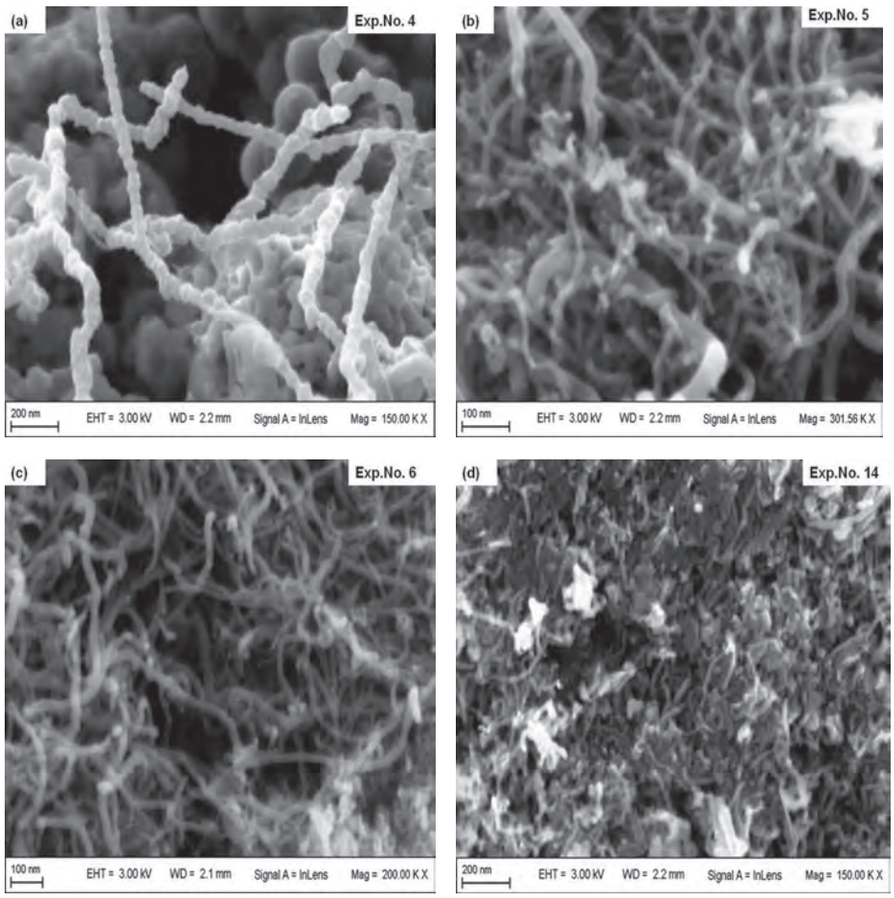

Fig. 2. FESEM images of MWCNTs.

of the temperature and process time were also found to be significant.

From the perturbation plot, the effect of CVD process parameters on the mean diameter of MWCNTs could be understood as described below;

(i) If the reaction temperature increases, the mean diameter of MWCNTs increases.

(ii) If the flow rate of precursor gas increases, the mean diameter of MWCNTs increases.

(iii) If the process time increases, the mean diameter of MWCNTs decreases.

Picher et al.[27] confirmed this above trend that at higher temperature, catalyst particles coarsening causes the disappearance of smallest catalyst particles and that led to increase in MWCNTs diameter; at higher precursor gas pressure the catalyst particles preferably covered by disordered carbon structures; which is clearly evident from the Figure 2(a). Navas et al.[28] proposed that the absence of small diameter CNTs in the short synthesis time, but parallel short synthesis time results in large decoration of carbon structures on to the catalyst, hence the longer synthesis

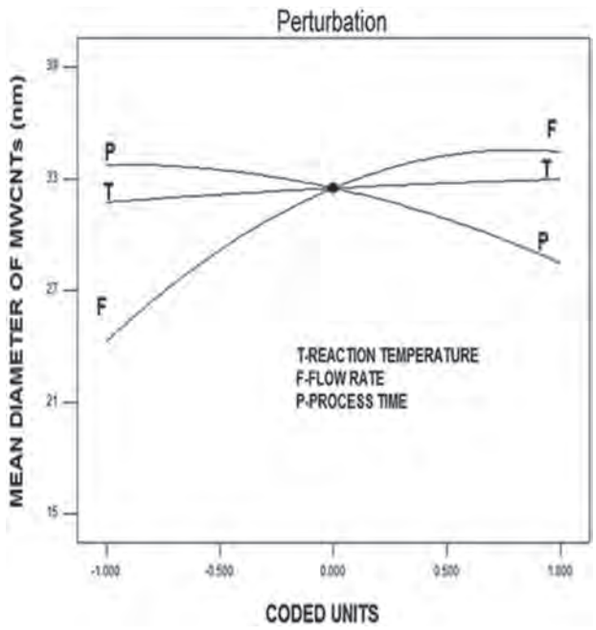

Fig. 3. Perturbation graph.

time results in smaller diameter of MWCNTs, which was clearly evident from the Figure 2(c).

5. PROCESS OPTIMIZATION

To obtain the optimized CVD process parameters and also to study the interaction effect of parameters on the response, the following three steps were followed,

Step 1: Numerical optimization
Step 2: Graphical optimization
Step 3: Point prediction.

The numerical optimization process is used to set the goals for each response to generate optimal conditions. The goal is fixed minimum to the responses and in range of the factors, in order to achieve minimum diameter of MWCNTs. The graphical optimization is used to set minimum to maximum limits for each responses in order to craft the superimpose graph highlighting an area of operability. The point prediction is used to enter the desired operating conditions and discover the predicted response values confidence intervals.

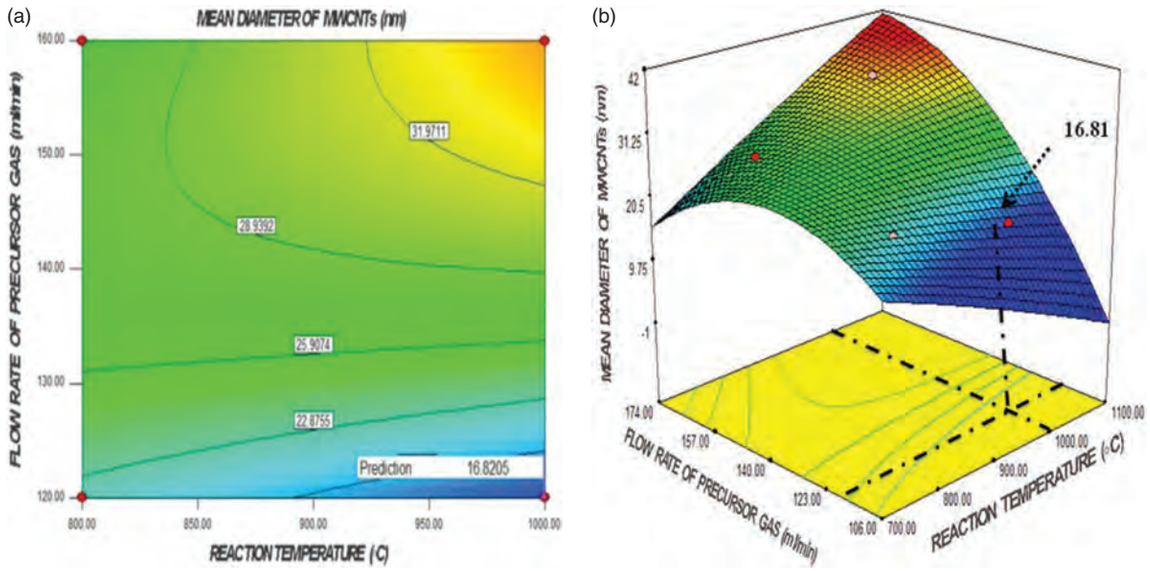

Fig. 4. Interaction effect of reaction temperature and flow rate of precursor gas (a) surface plot, (b) contour plot.

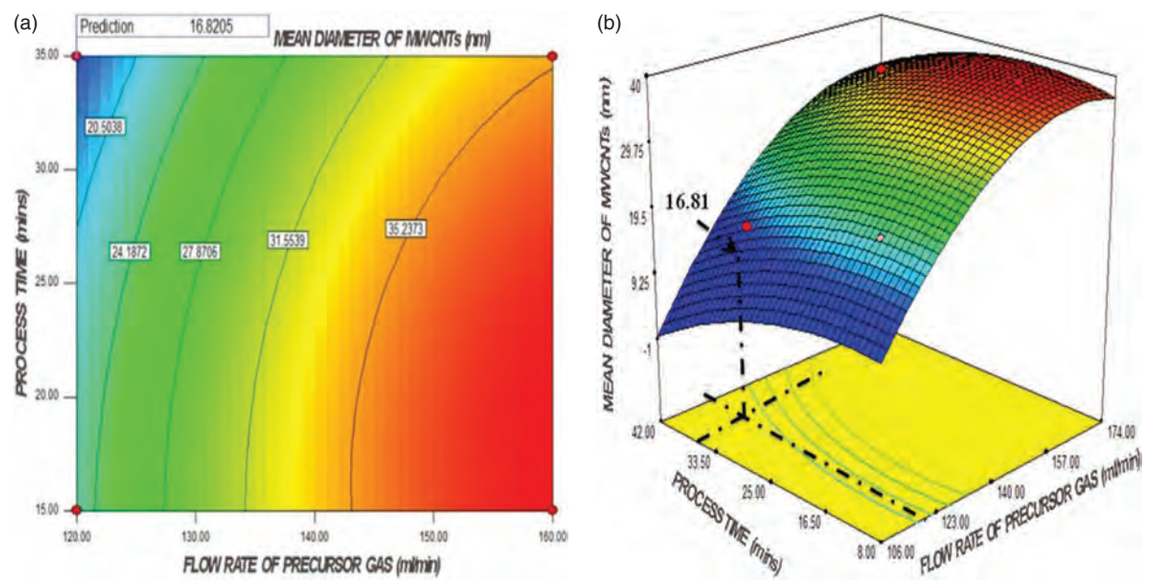

Fig. 5. Interaction effect of flow rate of precursor gas and process time (a) surface plot (b) contour plot.

Table IV. Validation test results.

Reaction temperature (°C)	Flow rate of precursor gas ml/min	Process time (mins)	Average diameter of MWCNTs (nm)
1. 1068	140	25	32
2. 1000	120	35	17
3. 900	160	5	32
4. 800	174	15	25

The developed empirical relationship (Eq. (6)) can be graphically illustrated by plotting contour and surface plots, as shown in Figures 4 and 5. In each contour and surface plot, two process variables are on the horizontal and vertical axis, with the third process variable remains constant at a specific level, and the response as a function of each process variable pairs filled the graphical area. Figures 4(a) and (b) show the responses of mean diameter of MWCNTs (nm) as a function of reaction temperature and flow rate of precursor gas, while the process time remains constant. The predicted mean diameter of MWCNTs was 16.81 nm and the actual diameter of MWCNTs was 17 nm, so the tolerance difference was more nearer.

From Figure 4(a) one can observe that the increase in reaction temperature leads to decrease in mean diameter of CNTs, on the other hand higher flow rate leads to increase in the mean diameter of CNTs. The surface plot (Fig. 4(b)) clearly reveals that the increase in reaction temperature minimizes the mean diameter of CNTs (with decrease in flow rate of precursor gas), due to the minimum amount of precursor gas flow and minimum pyrolysis of carbon diffusion towards the catalyst particle. The diameters of MWCNTs increases with the decrease in the precursor gas flow rate (Fig. 5(a)), with increase in the process time were clearly evident in the contour plot. The maximum mean diameter of MWCNTs reaches an apex (Fig. 5(b)) at the higher flow rate and an apex steep down to towards the minimum diameter, were the flow rate of precursor gas is minimum, while the reaction time is maximum. The long reaction duration, higher reaction temperature and medium flow rate of precursor gas tends to grow smaller diameter MWCNTs, with minimum side wall defects and presence of amorphous carbon were clearly evident in the Figure 2(c) (Exp. No. 6). The low reaction duration, higher reaction temperature and higher flow rate of precursor gas led to the growth of larger diameter MWCNTs, with side

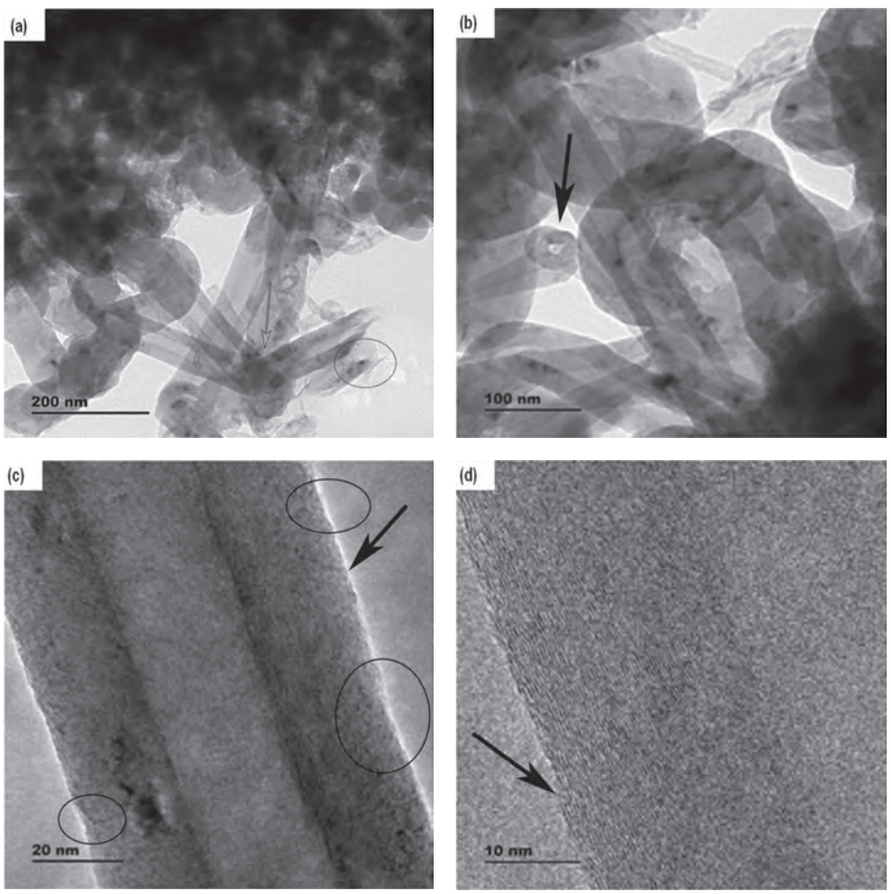

Fig. 6. Higher magnification (HRTEM) image of MWCNTs (Fig. 2(c)).

wall defects and presence of amorphous carbon in the side walls of CNTs were also high, were clearly evident in the Figure 2(a) (Exp. No. 4).

The validation test was carried out to check the novelty of developed empirical relationship, so the test was conducted by selecting the CVD process parameters within the feasible working limits. From the Table IV, it is clearly evident that the higher reaction temperature, medium flow rate of precursor gas and higher process time led to the growth of minimum diameter of MWCNTs.

6. CHARACTERISTICS OF MWCNTs

The high resolution transmission electron microscopy (HRTEM) analysis was carried out to study the characteristics of MWCNTs samples grown on optimized parameter condition. The HRTEM image is used to count the number of walls and to identify sidewall defects of CNTs. The Figure 6 shows the high resolution transmission electron microscopy (HRTEM) image of Figure 2(c) (Exp. No. 6). The Figure 6(a) shows the carbon samples reacting with source electrons from HRTEM (indicated by circle). In the image (Fig. 6(a)), MWCNTs bend severely due to forcible acid treatment (indicated by an arrow). The severe acid treatment tend to modify the string shaped CNTs to circular shape or angular shape CNTs.[29] The arrow shows the open ended (Fig. 6(b)) MWCNT tail, the open end tip clearly concludes the growth mechanism of MWCNTs was tip growth mode. The Figure 6(c) shows the MWCNT and the red circle indicates the presence of side wall defects and the arrow highlights the presence of amorphous carbon. The number of (Fig. 3(d)) concentric walls may vary from 30 to 35 and the red arrow indicates the presence of amorphous carbon in the side wall of MWCNTs.

7. CONCLUSIONS

The use of design of experiments tied with optimizing analysis is the effective way to develop an accurate output data and also effective way to reach the high end optimized CVD process parameters. Based on this investigation, the following conclusions are derived:

(i) An empirical relationship was developed to predict (at 95% confidence level) the mean diameter of MWCNTs synthesized via CVD process. The relationship was developed by incorporating CVD process parameters (reaction temperature, flow rate of precursor gas, process time) and mean diameter of MWCNTs.

(ii) From the ANOVA results, it is found that the flow rate of precursor gas is having predominant effect ($F = 619.60$) and reaction temperature is having less significant effect ($F = 8.95$) on the formation of MWCNTs and their diameters.

(iii) MWCNTs with minimum mean diameter of 16.8 nm were obtained under the CVD processing conditions of 1000 °C reaction temperature, 120 ml/min precursor gas flow rate, 35 min process time and the validation result adds additional novelty to the developed statistical model.

Acknowledgments: The first author gratefully acknowledges the financial support provided by M/s. VB Ceramics Consultants (VBCC), Nehru Nagar Industrial Estate, Kottivakkam, Chennai-600041, India through VBCRF (VB CERAMICS RESEARCH FELLOWSHIP). The authors are grateful to The Director, Naval Materials Research Laboratory (NMRL), DRDO, Ambernath, Maharastra for permitting to utilize FESEM facility to characterize MWCNTs. The authors are grateful to the Director, PSG Institute of Advance Studies, Coimbatore, Tamil Nadu for permitting to carry out HRTEM analysis.

References and Notes

1. M. De Volder, S. Tawfick, R. Baughman, and A. Hart, *Science* 339, 535 (**2013**).
2. B. Peng, M. Locascio, P. Zapol, S. Li, S. L. Mielke, G. C. Schatz, and H. D. Espinosa, *Nat. Nanotechnol.* 8, 628 (**2008**).
3. A. D. Franklin, M. Luisier, S. Han, G. Tulevski, C. M. Breslin, L. Gignac, M. S. Lundstrom, and W. Haensch, *Nano Lett.* 12, 758 (**2012**).
4. Q. Zhang, J. Huang, M. Zhao, W. Qian, and F. Wei, *ChemSusChem.* 4, 864 (**2011**).
5. W. Bauhofer, J. Z. Kovacs, and T. Swan, *Compos. Sci. Technol.* 69, 1486 (**2009**).
6. P. Taylor, A. Beigbeder, P. Degee, S. L. Conlan, R. J. Mutton, A. S. Clare, M. E. Pettitt, M. E. Callow, and J. A. Callow, *Biofouling* 24, 291 (**2011**).
7. M. Yu, *Science* 287, 637 (**2000**).
8. J. L. Hutchison, N. A. Kiselev, E. P. Krinichnaya, A. V. Krestinin, R. O. Loutfy, A. P. Morawsky, V. E. Muradyan, E. D. Obraztsova, J. Sloan, and S. V. Terekhov, *Carbon NY* 39, 761 (**2001**).
9. J. Chrzanowska, J. Hoffman, A. Małolepszy, M. Mazurkiewicz, T. A. Kowalewski, Z. Szymanski, and L. Stobinski, *Phys. Status Solidi* 252, 1860 (**2015**).
10. M. Kumar and Y. Ando, *Carbon NY* 43, 533 (**2005**).
11. K. J. Mackenzie, O. M. Dunens, and A. T. Harris, *Ind. Eng. Chem. Res.* 49, 5323 (**2010**).
12. J. Kong, A. M. Cassell, and H. Dai, *Chem. Phys. Lett.* 292, 567 (**1998**).
13. C. N. He, N. Q. Zhao, C. S. Shi, and S. Z. Song, *J. Alloys Compd.* 489, 20 (**2010**).
14. G. Atthipalli, R. Epur, P. N. Kumta, B. L. Allen, Y. Tang, A. Star, and J. L. Gray, *Thin Solid Films* 519, 5371 (**2011**).
15. S. Shukrullah, N. M. Mohamed, M. S. Shaharun, and M. Y. Naz, *Mater. Manuf. Process.* 31, 1537 (**2016**).
16. Z. Cao, Z. Sun, P. Guo, and Y. Chen, *Front. Mater. Sci. China* 1, 92 (**2007**).
17. R. Szabo and I. Kiricsi, *Carbon* 43, 2842 (**2005**).
18. W. Liu, A. Aziz, S. Chai, A. R. Mohamed, and C. Tye, *Can. J. Chem. Eng.* 90, 489 (**2012**).
19. D. C. Montgomery, Design and Analysis of Experiments, JohnWiley & Sons, Inc., New York (**2001**).
20. A. Nourbakhsh and B. Ganjipour, *Nanotechnology* 18, 115715 (**2007**).
21. G. Allaedini, S. Masrinda, and P. Aminayi, *Diam. Relat. Mater.* 66, 196 (**2016**).
22. S. Ã. Porro, S. Musso, M. Giorcelli, A. Chiodoni, and A. Tagliaferro, *Physica E* 37, 16 (**2007**).

RESEARCH ARTICLE

23. T. D. Makris, L. Giorgi, R. Giorgi, N. Lisi, and E. Salernitano, *Diam. Relat. Mater.* 14, 815 **(2005)**.
24. B. H. Guan, I. Ramli, N. Yahya, and L. K. Pah, *IOP Conf. Ser. Mater. Sci. Eng.* 17, 012 **(2011)**.
25. J. Zheng, R. Bao, J. H. Yi, and P. Yang, *Diam. Relat. Mater.* 68, 93 **(2016)**.
26. X. Ling, Y. Wei, L. Zou, and S. Xu, *Appl. Surf. Sci.* 276, 159 **(2013)**.
27. M. Picher, E. Anglaret, R. Arenal, V. Jourdain, L. Colloïdes, and V. Nanomat, *ACS Nano* 5, 2118 **(2011)**.
28. H. Navas, M. Picher, A. Andrieux-Ledier, T. Michel, A. Kozawa, T. Maruyama, E. Anglaret, A. Loiseau, and V. Jourdain, *ACS Nano* 276, 159 **(2017)**.
29. J. Song, S. Feng, J. Zhao, J. Zheng, and Z. Zhu, *Mater. Res. Bull.* 45, 1234 **(2010)**.

Received: 5 December 2017. Accepted: 8 January 2018.